Adaptable Pulse Compression in φ-OTDR With Direct Digital Synthesis of Probe Waveforms and Rigorously Defined Nonlinear Chirping

Y. Muanenda, S. Faralli, C. J. Oton, P. Velha, and F. Di Pasquale

***Abstract*—Recent research in Phase-Sensitive Optical Time Doman Reflectometry (φ-OTDR) has been focused, among others, on performing spatially resolved measurements with various methods including the use of frequency modulated probes. However, conventional schemes either rely on phase-coded sequences, involve inflexible generation of the probe frequency modulation or mostly employ simple linear frequency modulated (LFM) pulses which suffer from elevated sidelobes introducing degradation in range resolution. In this contribution, we propose and experimentally demonstrate a novel φ-OTDR scheme which employs a readily adaptable Direct Digital Synthesis (DDS) of pulses with custom frequency modulation formats and demonstrate advanced optical pulse compression with a nonlinear frequency modulated (NLFM) waveform containing a complex, rigorously defined modulation law optimized for bandwidth-limited synthesis and sidelobe suppression. The proposed method offers high fidelity chirped waveforms, and when employed in resolving a 50-cm event at ∼1.13 km using a 1.2-μs probe pulse, matched filtering with the DDS-generated NLFM waveform results in a significant reduction in range ambiguity owing to autocorrelation sidelobe suppression of ∼20 dB with no averages and windowing functions, for an improvement of ∼16 dB compared to conventional linear chirping. Experimental results also show that the contribution of autocorrelation sidelobes to the power in the compressed backscattering responses around localized events is suppressed by up to ∼18 dB when advanced pulse compression with an optical NLFM pulse is employed.**

***Index Terms*—Coherent effects, fiber nonlinear Optics, fiber optic systems, pulse compression, scattering.**

I. Introduction

RECENTLY, distributed optical fiber sensors with enhanced measurement features have been a subject of wide research and development thanks to their application in safety and integrity monitoring in many areas including the transportation, infrastructure, energy and security industries. Measurements in such sensors are based on the observation of Raman, Brillouin or Rayleigh scattering in an optical fiber, which are sensitive to local changes in physical parameters [1]. Specifically, coherent Rayleigh scattering is employed in Distributed Acoustic Sensing (DAS) for measurements of disturbances such as intrusions and vibrations in the vicinity of the fiber. While there are many schemes employing signal processing in the frequency and correlation domains, a commonly employed technique for DAS is Phase-sensitive Optical Time domain Reflectometry (φ-OTDR) [2]. When a pulse of light from a coherent laser propagates in an optical fiber, the resulting coherent Rayleigh scattering exhibits coherent speckles, which are sensitive to the change in vibration or temperature at each point along the fiber. A disturbance occurring at a specific location induces a change in the optical path length of the fiber. This in turn changes the phase of the backscattered light within the pulse width, which is observed either in the change in intensity or the actual phase of the photodetected signal at the receiver. Many investigations have been devoted to the enhancement of the performance of conventional φ-OTDR in recent years, including increasing dynamic capacity, improving quantitative measurement precision [3], suppressing fading, extending sensing distance and measurand dynamic range and enabling more spatially resolved sensing [4].

Specifically, investigations on enhanced range resolution are driven by requirements in specific areas of applications such as structural health monitoring of bridges, dams or pipelines, condition monitoring of wind turbines [5], hot-spot detection in steam power generation schemes [6] and along power cables. Commonly, multiple FBGs laid in close proximity and interrogated in different channels are used in such systems [7]. Spatially resolved sensing using φ-OTDR schemes is also highly desirable in monitoring scenarios such as perimeter security. Fiber-based solutions for such systems, which are commonly known as Perimeter Intrusion Detection Systems (PIDS) have been mostly implemented using Fiber-Bragg Grating sensors [8], [9], whose effective use requires multiplexed configurations usually put in meshes of closely spaced gratings requiring independent, multi-channel interrogation which must scale with the length of the perimeter. Although optical frequency domain reflectometry (OFDR) and optical correlation domain reflectometry (OCDR) techniques offer enhanced spatial resolution, the basic sensing mechanism in these systems is such that, due to frequency sweeping, there is a strict tradeoff between measured response dynamics and sensing distance. One of the techniques to improve the spatial resolution of φ-OTDR is the use of linear frequency modulation (LFM) within the duration of the pulse, and subsequent matched filtering to obtain compressed responses

Manuscript received October 17, 2021; revised February 8, 2022; accepted February 14, 2022. Date of publication February 22, 2022; date of current version March 16, 2022. *(Corresponding author: Yonas Muanenda.)*

The authors are with the Optical Fiber Sensors group of Institute of Mechanical Intelligence, Scuola Superiore Sant'Anna, 56127 Pisa, Italy (e-mail: y.muanenda@santannapisa.it; s.faralli@santannapisa.it; c.oton@santannapisa.it; philippe.velha@santannapisa.it; f.dipasquale@sssup.it).

Digital Object Identifier 10.1109/JPHOT.2022.3152816

[10], [11]. However, LFM probes have sidelobes in their Autocorrelation Functions (ACFs), which introduce ambiguity in range resolution during pulse compression [12].

To suppress error-inducing sidelobes in the ACFs, thousands of averages in the order of 10000 were needed [4], significantly reducing the useable sampling rate, or other techniques such as apodization need to be employed. A technique used to improve the SNR in φ-OTDR using chirped-pulse amplification has also been proposed [13], where a narrow pulse is allowed through a chirping medium, which stretches the pulse energy over a longer temporal range, and another medium with reverse dispersion characteristics offsets the effect of dispersion while retaining the net gain in SNR. The repetition rate of the source for the short pulses, which is in the order of 10 MHz, limited the reported sensing range to 10 m. A method for spatially resolved measurement with sidelobe suppression using a Gaussian probe pulse with an LFM waveform has been demonstrated, and comparison of compressed backscattering responses shows that such a probe yields an improvement of 13 dB compared to a square pulse of an equivalent bandwidth [21]. Still, the frequency modulation law used in each type of pulse is linear with inevitable sidelobes in its autocorrelation and compressed backscattering response. Another approach used for the suppression of sidelobes is the use of perfect periodic binary phase codes [22]. More specifically, the use of a specific family of perfect periodic codes, called bi-phase Legendre sequence, of 6211 pulses coupled with a polarization diversity scheme has been shown to provide low probability of fading with high scan rate, enhanced dynamic range and sub-meter resolution, with reported sensing distance of 144 m [23]. The choice of such bi-phase sequences is driven to a large part by the simplicity of their generation and subsequent piggybacking on an optical carrier and, in general, longer codes are needed to achieve higher energy efficiency and compression ratio [24].

A related study shows that suppression of common mode phase drift noise in a coherent φ-OTDR scheme is possible using a dual-sideband LFM probe containing chirps with opposite slopes at the two sides of the carrier [25]. More recently, frequency multiplexing wherein a train of frequency shifted pulses is used to probe the fiber has been combined with a polarization diversity receiver, not only to address fading but also to significantly suppress measurement noise and increase linearity, offering measurements with a minimum detectable strain of 0.6 $p\varepsilon/\sqrt{Hz}$ at 10 km distance and a spatial resolution of 10 m [26]. The use of probes containing more complex waveforms with Nonlinear Frequency Modulation (NLFM), which have been employed to achieve suppressions of the sidelobes in radiofrequency electronic systems [14], offers specific advantages. A long-range phase-OTDR which avoids the use of distributed amplification based on multi-carrier NLFM has been reported [27]. However, although a long sensing range is achieved using this method, the reported spatial resolution is 2.7 m and this contribution is particularly focused on mitigation of fading and transient effects and the proposed frequency modulation law is not optimized for bandwidth limited synthesis, which is highly desirable in the actual realization of the technique with cost-effective interrogators combining digitizers and synthesizers in a single compact device [18]. The clear impact of linear and nonlinear chirping of probes on both the autocorrelations of optical pulses (not digital or RF ones) and the real impact on the amplitude and power of compressed coherent Rayleigh backscattering responses have not been closely studied as well. Moreover, it is highly desirable to employ direct digital synthesis of custom, rigorously defined frequency modulation laws. Most of the schemes implemented so far employ phase coding and/or frequency modulation schemes whose precise features are closely tied to specific optical or electronic components used for pulse waveform shaping and their detailed characteristics cannot be easily reprogrammed to benefit from highly desirable features which come from rigorously defined and adaptable frequency or phase modulation laws optimized for advanced matched filtering.

There have been a number of methods to generate frequency modulated signals, including the three-segment chirp function [15], arctan and Zak-transform [16] techniques. The optical fiber sensing community can benefit from further research on new schemes for easily adaptable use of NLFM waveforms in probes for spatially resolved optical reflectometry, including tools to compare the achievable range resolution qualities of different optical pulse compression techniques.

Until recently, one of the hurdles of generating optical probe pulse waveforms with flexible frequency modulation has been the challenge in the synthesis of custom analog waveforms from digital ones for modulation on an optical carrier. Yet, during the last decade, there have been rapid technological advancements in digital-to-analog converter (DAC) systems which enabled their use in high-speed optical communication systems and radiofrequency applications for flexible digital signal processing [17]. This is thanks to the wider development and commercial availability of compact DDS devices, including DAC and analog-to-digital (ADC) systems for signal generation, acquisition and processing in one module, with optimizations for low power consumptions [18]. Hence, it would be desirable to employ such cost-effective schemes in advanced matched filtering techniques for optical pulse compression, where the input waveform for interrogation can be custom-designed as per desired modulation features. The flexibility not only enables generation of complex waveforms difficult to realize with simple opto-electronic components but also offers dynamic adaptation of the probe waveform generation to specific sensing conditions. Since there is a less stringent dependence of the probe type with the sensing scheme, flexible matched filtering with DDS makes it easy to quickly switch measurement resolutions even in between different acquisitions of a measurement session and use probes which provide additional features.

In this contribution, we show that chirping of the probe in a φ-OTDR can be done in a flexible and programmable manner using Direct Digital Synthesis of desired pulse frequency modulation, and demonstrate the implementation of an easily adaptable, rigorously defined NLFM-based φ-OTDR system for effective disambiguation [19]. We demonstrate that compressed responses with readily adaptable, DDS-generated linear chirping enable measurements at resolution values down to 50 cm using a 1.2-μs pulse of 500 MHz bandwidth, offering a pulse

compression ratio of ∼240 with no averaging of acquired traces. When employed in advanced filtering using NLFM probe with a complex, rigorously defined modulation law optimized for bandwidth-limited synthesis, the flexibility of the DDS scheme offers significantly higher disambiguation in the backscattering response of events separated by 50 cm at ∼1.13 km. This is thanks to the sidelobe suppression in the ACF of the NLFM being ∼20 dB, which is an improvement of ∼16 dB compared to that of a conventional LFM pulse. We also confirm the reduction of ambiguity with NLFM using a quantitative, power-vs-range analysis of two closely spaced events which shows the benefits of a rigorously defined NLFM chirp in suppressing the power in sideways oscillations in compressed backscattering responses by up to ∼18 dB.

The rest of the article is organized as follows: The theory of matched filtering used in the customizable pulse compression and the NLFM pulse waveform's frequency modulation law is given in Section II. An outline of the experimental setup used to demonstrate the proposed scheme is provided in Section III, which is followed by the experimental results and discussions in Section IV.

II. Theory

The enhancement of the range resolution using frequency modulation of a pulse in a generic reflectometry technique hinges on the method of matched filtering. To understand this technique, let us assume the system at the receiver of a generic back-reflected signal x(t) is defined by a filter having an impulse response of h(t) and y(t) is the signal at the output, as shown in Fig. 1(a). If x(t) is the result of the propagation of the back-reflected signal s(t) in a channel which adds additive white Gaussian noise (AWGN), the interest in matched filtering is to determine conditions which maximize the SNR of the filtered signal at a given time instance t_M, which in time and frequency domain will be:

$$y(t) = x(t-t_M) \otimes h(t) \Leftrightarrow Y(\omega) = X(\omega)e^{j\omega t_M}H(\omega) \quad (1)$$

The power of the signal at the output of the receiver will then be given by [12]:

$$P_s = \left|\frac{1}{2\pi}\int_{-\infty}^{\infty} X(\omega)H(\omega)e^{j\omega t_M}d\omega\right|^2 \quad (2)$$

If the power spectral density of the AWGN is $N_0/2$ at the input of the receiver, the output will be given by $N_0/2\ |H(\omega)|^2$. The power of the noise then becomes:

$$P_N = \frac{1}{2\pi}\frac{N_0}{2}\int_{-\infty}^{\infty}|H(\omega)|^2 d\omega \quad (3)$$

The SNR at the output of the receiver filter, which is the ratio of the total power of the signal to that of the noise given in equations (2) and (3) can be given by:

$$SNR = \frac{\left|\frac{1}{2\pi}\int_{-\infty}^{\infty} X(\omega)H(\omega)e^{j\omega t_M}d\omega\right|^2}{\frac{1}{2\pi}\frac{N_0}{2}\int_{-\infty}^{\infty}|H(\omega)|^2 d\omega} \quad (4)$$

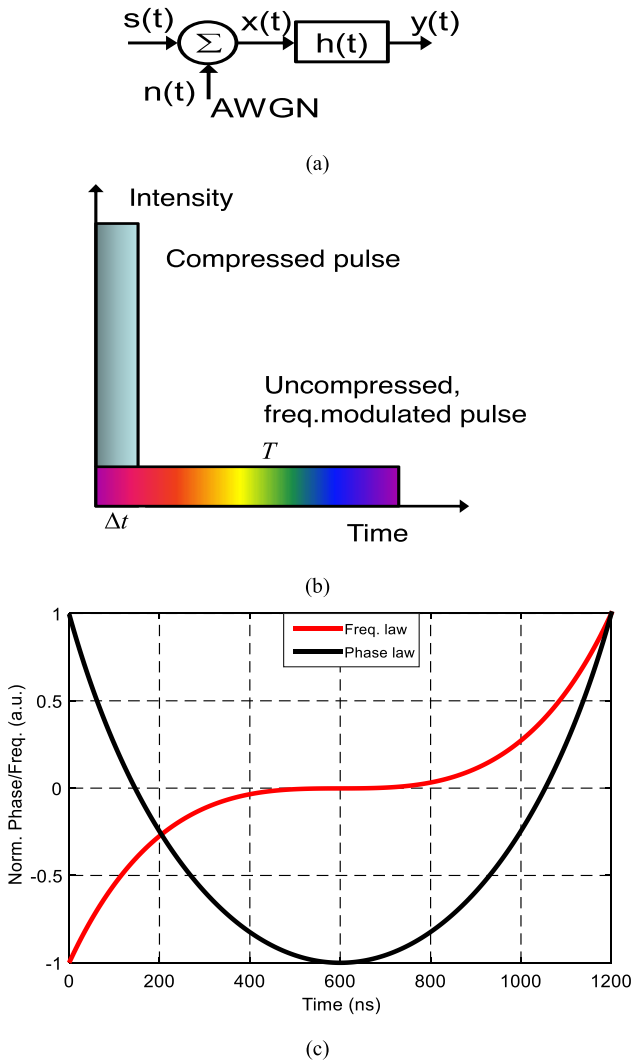

Fig. 1. (a) Schematic of a matched filter. (b) Mechanism of a generic pulse compression with frequency modulation. (c) Phase and frequency modulation laws for NLFM pulse used in proposed scheme.

To determine the characteristics of the filter which maximize the SNR at t_M, first we note that, for any two signals $x_1(t)$ and $x_2(t)$ with FFTs $X_1(\omega)$ and $X_2(\omega)$, respectively, one of many forms of Schwartz's inequality can be written as:

$$\left|\int_{-\infty}^{\infty} X_1(\omega)X_2(\omega)d\omega\right|^2 \leq \left|\int_{-\infty}^{\infty} X_1(\omega)d\omega\right|^2\left|\int_{-\infty}^{\infty} X_2(\omega)d\omega\right|^2 \quad (5)$$

When applied to the numerator of (4), the inequality in the SNR becomes [12]:

$$SNR \leq \frac{\left[\frac{1}{2\pi}\right]^2\int_{-\infty}^{\infty}|X(\omega)|^2 d\omega\int_{-\infty}^{\infty}|H(\omega)|^2 d\omega}{\frac{N_0}{4\pi}\int_{-\infty}^{\infty}|H(\omega)|^2 d\omega} \quad (6)$$

The numerators in (4) and (6) are equal when the filter response is such that $H_M(\omega) = \alpha X*(\omega)\exp(-j\omega t_M)$ for an arbitrary constant α, which means $h(t) = \alpha x*(t_M\text{-}t)$. Namely, the filter is a

mere inverse conjugate of the scaled and delayed version of the input signal itself and hence is said to be matched to the input at the receiver. If the filter response which maximizes the SNR is substituted in (6), the SNR becomes:

$$SNR_{\max} = \frac{\left[\frac{1}{2\pi}\right]^2 \int_{-\infty}^{\infty} \left|\alpha |X(\omega)|^2 d\omega\right|^2,}{\frac{N_0}{4\pi} \int_{-\infty}^{\infty} |\alpha X * (\omega) \exp(-j\omega t_M)|^2 d\omega}, \quad (7)$$

where the $|X(\omega)|^2$ in the numerator resulted from the multiplications of $X(\omega)$ and its conjugate. After a single simplification and re-arrangement, the maximum SNR will be given by:

$$SNR_{\max} = \frac{2}{N_0}\left[\frac{1}{2\pi}\int_{-\infty}^{\infty} |X(\omega)|^2 d\omega\right] = \frac{2E}{N_0}, \quad (8)$$

where E is the total energy of the signal. Hence, it is evident that the maximum SNR at the output of the matched filter is dependent on the total energy of the signal, no matter what modulation scheme is used in the probe. It is worth noting that, when using matched filtering in reflectometry techniques, the process itself does not necessarily involve the design of a dedicated filter. It entails the processing of the signal with a response matched to the actual signal sent into the medium under test. For instance, when using OTDR in optical fiber, the waveform of the transmitted pulse with certain characteristics can be used as the impulse response of the matched filtering to maximize the SNR of the signal at the receiver. A commonly used matched filter is that of the LFM pulse in which the signal frequency varies linearly within the pulse duration. For an LFM pulse having a frequency per unit time ratio, also known as the chirp rate, of k and width T, the waveform is given by:

$$s(t) = rect(t/T) \exp\left[j2\pi(f_c t + {}^{k}/_{2}t^2)\right]. \quad (9)$$

When used in a generic reflectometry technique, the resulting output of the matched filter results in a convolution of the scaled amplitude response of the fiber A(t) with a sync-like function given by [10]:

$$\Theta(t) = \{rect\,(t/2T)\} \times \{T\sin[\pi kt\,(T-|t|)]/(\pi kTt)\}. \quad (10)$$

The spatial resolution of the response for an optical fiber as provided by the Rayleigh criteria, for $B = kT$, which is commonly known as the signal base, is given by:

$$z = \frac{c}{2nB}. \quad (11)$$

where c is the speed of light in free space and n is the group refractive index in the fiber. Hence, the spatial resolution of the obtained signal is dependent on the total bandwidth content as determined by the pulse width and chirp rate, as opposed to only the pulse width for conventional OTDR. Since there is more range resolution when using LFM, the result of matched filtering with enhanced resolution is also referred to as the compressed response of the pulse, as shown in the schematic in Fig. 1(b), which depicts the energy equivalence of a longer, chirped pulse and an equivalent narrower pulse obtained after matched filtering. When using NLFM, the frequency is chirped according to a certain nonlinear frequency modulation law which, thanks to the fact that the frequency and phase are differentiation-integration pairs, defines the phase modulation law. These are generally nonlinear functions whose precise features are determined by the parameter that needs to be optimized, which in our case is the sidelobe suppression feature. In our method, we have explored different techniques for pulse compression using NLFM and the chosen nonlinear frequency modulation scheme is optimized for bandwidth-limited synthesis and has the following characteristics [14]:

$$s(t) = A\left\{rect(\tfrac{t-T/2}{T})\right\} \times \exp\left[j2\pi\left(\tfrac{T\sqrt{\Delta^2+4}}{2\Delta} - \left[\tfrac{T^2(\Delta^2+4)}{4\Delta^2} - \left(t-\tfrac{T}{2}\right)^2\right]^{1/2}\right)\right], \quad (12)$$

where Δ and T are the nonlinear frequency span and the pulse width, respectively. The normalized frequency and phase modulation laws for the NLFM pulse used in our DDS-based phase OTDR are given in Fig. 1(c), which shows symmetric nonlinear curves with respect to the center of the pulse. It is evident that conventional chirping or frequency modulation methods cannot be employed to generate such a rigorously defined waveform.

It is also worth noting that, although analytic approximations of the ACF can be used to capture the features of the matched filter output, exact computation of the ACF for any generic probing waveform can best be obtained by making a direct numerical computations for both LFM and NLFM pulses. The choice of the NLFM waveform is made based on whether it gives sidelobe suppression with respect to the LFM both before and after digital synthesis. Note also that the synthesis of the LFM and NLFM waveforms is done by programmatically generating the respective functions as per their frequency modulation laws and parameters and subsequently loading them onto the DDS module.

III. Experimental Setup

The schematic of the experimental setup used to demonstrate the technique is given in Fig. 2. The part for the generation of the required pulse waveform is shown at the top, where the 99% tap of the continuous wave light from a coherent laser with a linewidth of 200 kHz is coupled to an I-Q modulator, which is a dual-parallel Mach-Zehnder Modulator (MZM) operated in Single Sideband Suppressed Carrier (SSB-SC) mode. The modulator has a nested Mach-Zehnder configuration with an outer interferometer comprised of two separate interferometers in each of its arms. Its bias point is controlled using three independent voltage inputs whose levels are carefully adjusted to obtain typical suppression values for the carrier and one sideband of more than 20 dB. This is possible thanks to the use of an electric hybrid which takes an RF signal at the input and gives rise to two orthogonal signals to feed the two inputs of the modulator. The input to the hybrid is fed through a three-stage broadband amplifier driven by a programmable DDS module with an embedded DAC having a sampling rate of 10 GS/s. The features of the signal from the DDS can be adapted to the desired pulse duration, repetition rate and phase or frequency

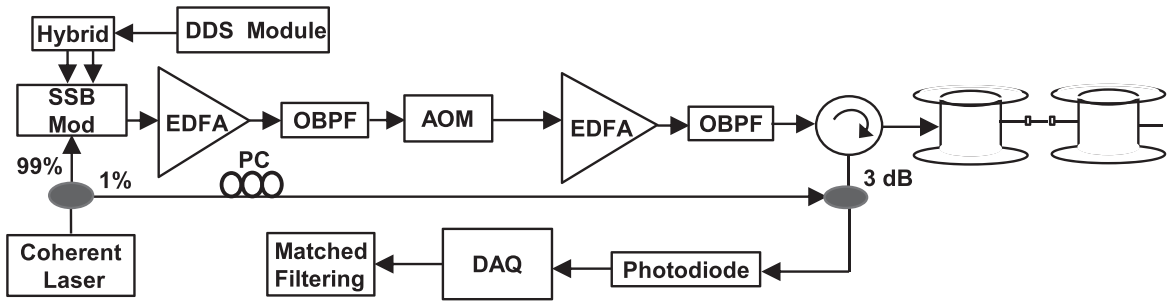

Fig. 2. Experimental setup.

modulation formats without changing other parameters in the physical setup.

Then, the frequency modulated SSB-SC signal from the modulator is first amplified using the Erbium-doped Fiber Amplifier (EDFA) and filtered using an Optical Bandpass Filter (OBPF) to suppress the Amplified Spontaneous Emission (ASE) noise. The signal is subsequently gated with a high-extinction ratio Acousto-optic Modulator (AOM) driven with a pulsed signal synchronized with the generated pulse format. The driving signal to the AOM is slightly delayed to account for the physical position of the AOM and SSB modulator in the setup. The signal is further boosted and filtered using a second pair of EDFA and OBPF before being fed to port 1 of the three-port circulator. The probe is subsequently sent into the Fiber Under Test (FUT), which is composed of two spools of fiber, FUT-1 and FUT-2, separated by patch cords of varying length. Since the aim is to demonstrate the use of DDS-generated frequency modulation of pulses to enhance range resolution, the sensor was used to accurately identify the position and length of the patch cords, which was narrowed from tens of meters down to 0.5 m. The coherent Rayleigh backscattering from the signal is then mixed with the 1% tap of the seed laser, which serves as a local oscillator with its polarization being adjusted using the polarization controller (PC) to mitigate the effect of fading, subsequently detected using a 10-GHz photodiode and acquired in real-time using an oscilloscope with a Data Acquisition board (DAQ) having a sampling rate of 10 GS/s.

Note that while other schemes involve the use of asynchronous matched filtering with the pulse waveform fed to the modulator of the optical wave, we employed synchronous matched filtering whereby the same mixing of a tap of the probe with the local oscillator has been used to characterize the probing pulses sent into the fiber. This way, the contributions of the optical components before the tap to the noises in the matched filter and uncompressed backscattering signals remain the same. The post-processing at the receiver involves matched filtering with the characterized pulse to obtain the compressed response. Such a method enables more denoising since the pulse compression, which involves correlation of the contaminated signal with an initial seed one serving as a matched impulse response, provides optimum improvement in SNR when the signal serving as a matched filter is taken as close as possible to the channel, which in our case is the fiber. This is done by choosing the optical pulse sent into the fiber as a matched filter, as opposed to the case for an asynchronous mode where the matched filter is the probe waveform before it is modulated on the optical carrier, amplified and filtered. Since the aim is to check the fidelity of the synthesized signal in the presence of noise as well as the result of compressed and uncompressed responses after matched filtering, no averages were performed on the acquired backscattering signal and characterized pulse.

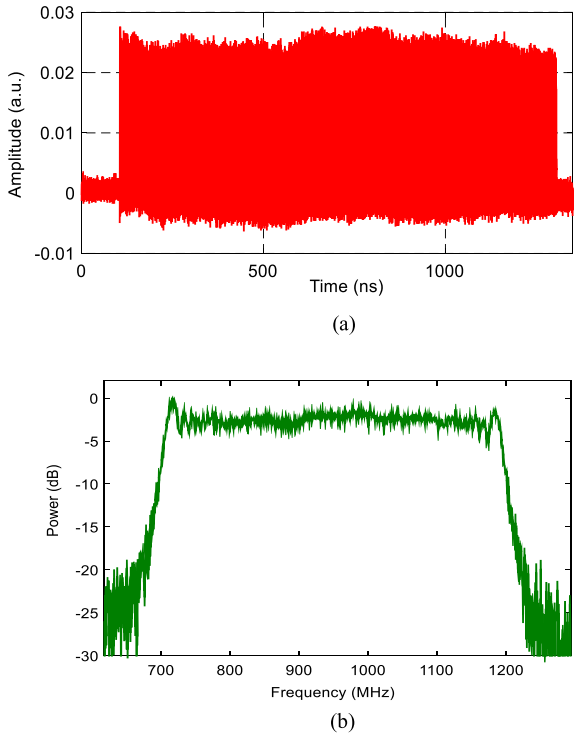

Fig. 3. (a) Synthesized LFM chirp in time domain, and (b) Chirp Spectrum.

IV. Experimental Results and Discussions

The first set of measurements performed involve the characterization of the ability of the DDS synthetization technique to generate chirp waveforms as per desired bandwidth and pulse duration in the presence of no averages. The plots in Fig. 3(a) and (b) show the time and frequency domain plots of an LFM pulse with a chirp bandwidth of 500 MHz and a temporal width of 1.2 μs, demonstrating the relative fidelity of the DDS technique

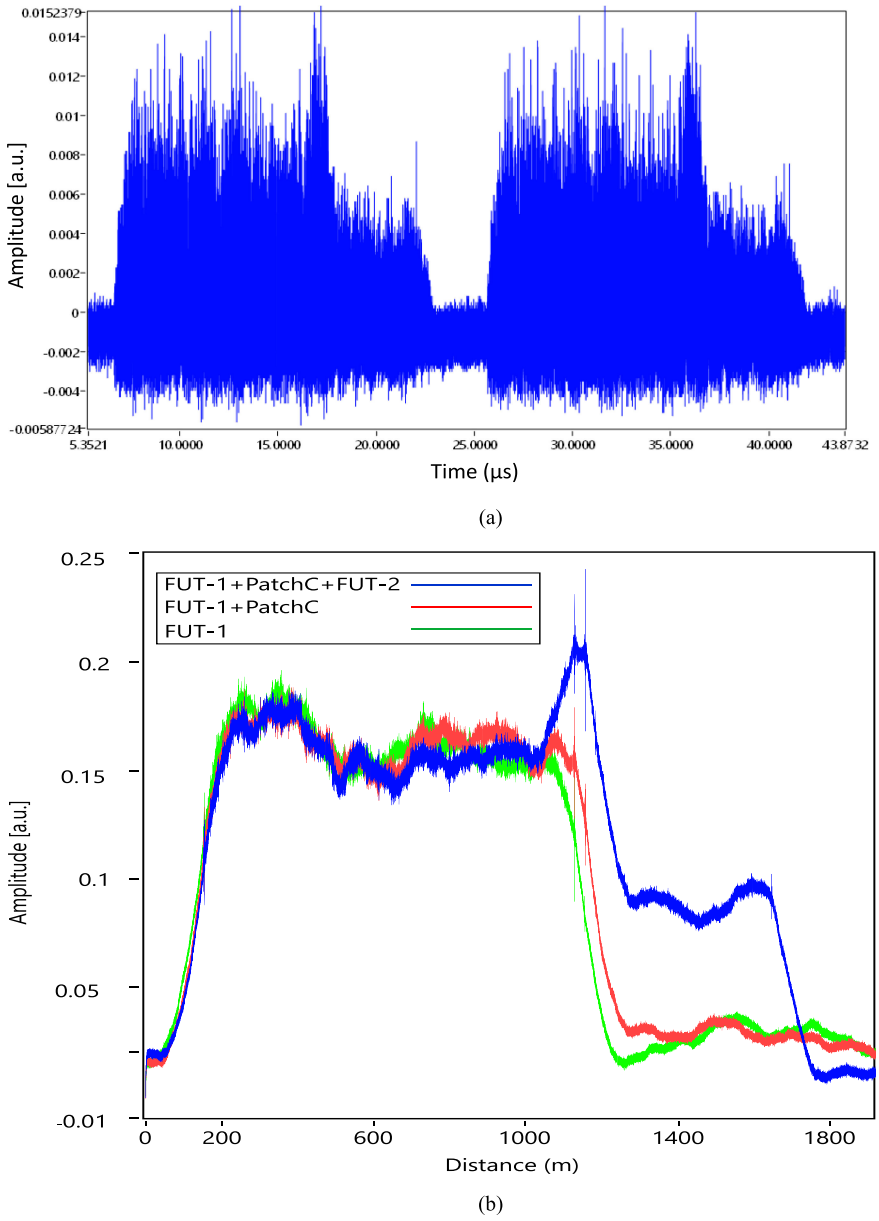

Fig. 4. (a) Raw backscattering response of the whole fiber with FUT-1 and FUT-2 connected with patch cord. (b) Compressed response with matched filtering for all three fiber spans when the patch cord is not connected at all (green), connected from one FUT-1 end (red), and then both ends (blue).

to keep the desired features of the generated analog signal and digitized optical pulse.

The compressed responses of the linear chirped probe have been studied for patch cords with different length down to 50 cm placed at ∼1.13 km. This method of determining the resolution is more effective compared to ones in conventional schemes based solely on the duration and/or total bandwidth content of the probing pulse alone, as the latter can lead to errors due to changes in pulses during propagation along the fiber.

Measurements of raw uncompressed backscattering traces were performed for three configurations: the first spool FUT-1 alone, connecting a patch cord at the end of FUT-1, and then adding FUT-2 so that the patch cord separates the two spools. For each case, the backscattering undergoes pulse compression using matched filtering with characterized chirped pulse sent into the fiber. A raw uncompressed trace showing the scenario where all of FUT-1, the patch cord and FUT-2 are connected is given in Fig. 4(a), where the patch cord is indistinguishable. Subsequently, the raw traces were compressed using the photodetected and digitized LFM pulse as a matched filter.

The compressed responses for the three sets of measurements are given in Fig. 4(b), which shows the compressed trace for just FUT-1 (green), FUT-1 with the patch cord (red) and with all three FUT-1, patch cord and FUT-2 connected (blue). In addition to the expected enhancement in SNR due to matched filtering, the reflections at the two ends of the patch cord are visible in the compressed responses despite the fact that the probing pulse has a much longer spatial width, thereby confirming the

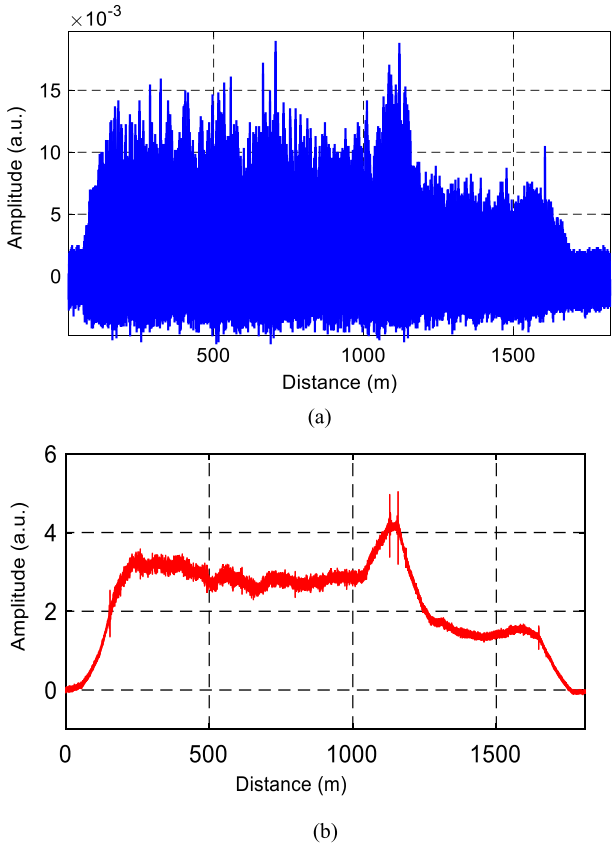

Fig. 5. Sample (a) Raw backscattering signal for one cycle and (b) Compressed backscattering response.

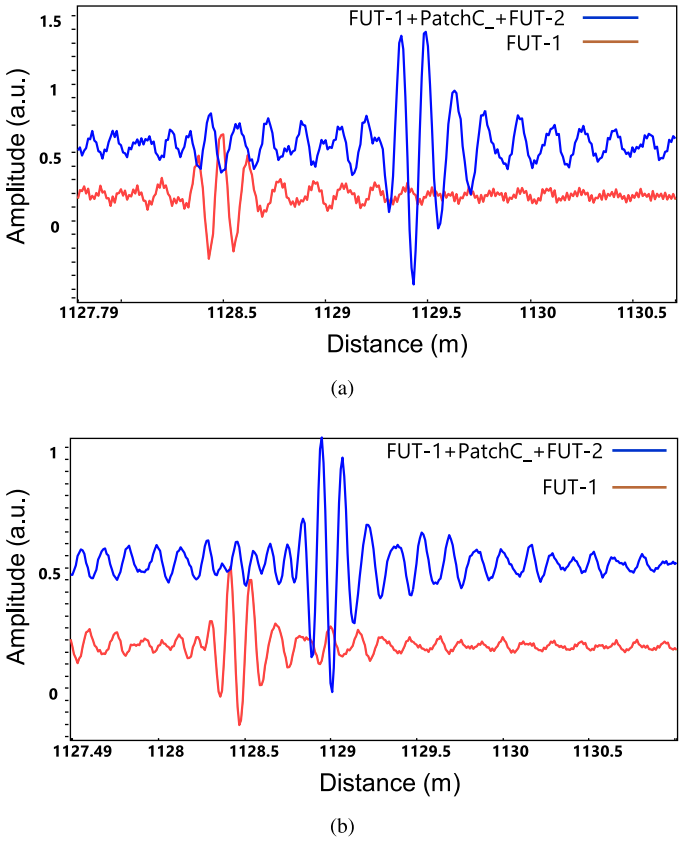

Fig. 6. LFM pulse compression for separate measurements of (a) 1-m and, (b) 0.5-m patch cord starting at 1128.5 m.

effectiveness of the pulse compression with a DDS-generated pulse.

A closer look at the raw φ-OTDR trace for one cycle of the FUT is shown in Fig. 5(a), and exhibits coherent speckles of the Rayleigh backscattering from both fiber spools. The compressed response is given in Fig. 5(b), where the position of the patch cord is clearly visible despite its length being much less than the spatial resolution of the probing pulse. This could not have been observed in conventional interrogation without frequency modulation, which offers a spatial resolution of 120 m when using 1.2 μs pulses.

To confirm the effectiveness of the matched filtering in determining the accurate position and length of events near the spatial resolution limit provided by pulse compression, patch cords with decreasing length have been put at 1128.5 m from the start of FUT-1. As shown in Fig. 6(a) and (b), the spans of the patch cords of length 1 m and 0.5 m with reflection events only at one connector end are clearly visible. Since the resolution of two events spaced 0.5 m apart would have required 5-ns pulses in the LFM probe, the proposed scheme offers an effective pulse compression ratio of ∼240. Note that the two measurements have been performed in separate instances with synchronous matched filtering employed with the optical pulse sent into the fiber being used as a matched filter after photodetection and subsequent digitization in each case.

The exact feature of another sample response from a 50-cm span with reflection events which have been deliberately induced

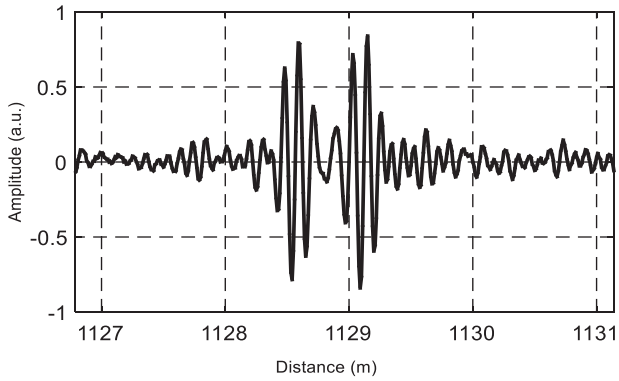

Fig. 7. Compressed LFM response for measurement of a 50-cm patch cord span.

at both connector ends by slightly adjusting each one, is clearly visible in Fig. 7, which also shows that the compressed trace exhibits a non-localized, sinc-like pattern due to the sidelobes resulting from the use of the LFM probe, consistent with similar observations in RF applications.Note that the effective suppression of sidelobes in compressed LFM pulse responses in scenarios where no averaging has been used can be significantly degraded from the ideal values at times going down to a few dB, as has been demonstrated in optical LIDAR systems [20].

Besides incurring relative ambiguity of a response which is happening at the granularity of the achievable spatial resolution, such a measurement incurs errors in measured signal intensity

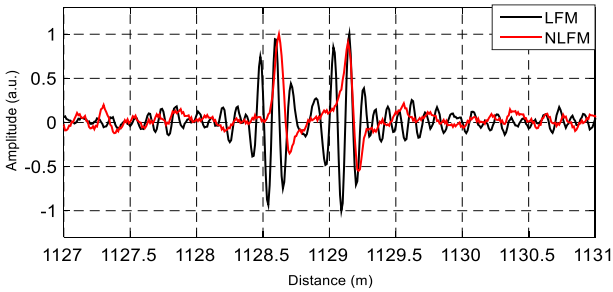

Fig. 8. Compressed backscattering responses near 50-cm patch chord span when using NLFM and LFM probes.

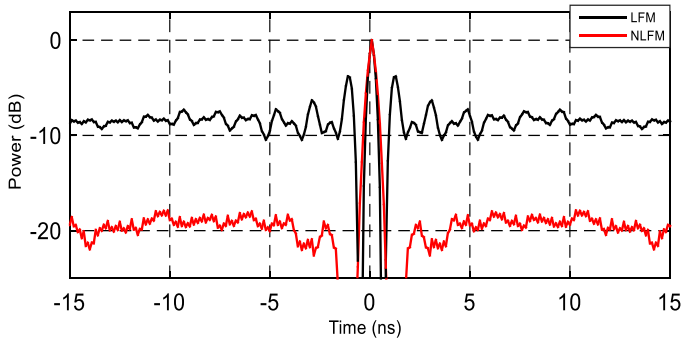

Fig. 9. Comparison of the relative power levels at the peak and sidelobes in autocorrelation functions of LFM and NLFM pulses used in respective matched filters.

of the backscattering from a single event which is clearly known to occur at a fixed position of the connector. In addition, when measuring vibrations from localized sources which in general leave spatially dispersed footprints, such ambiguity might result in the same local disturbance inducing different compressed responses from points within the spatial resolution. This contributes to errors in spatially sampled or averaged amplitude or phase responses of more complex events in a φ-OTDR, resulting in nonlinear responses not necessarily corresponding to the external impact.

To address this issue, we employed advanced matched filtering with an NLFM pulse whose modulation and frequency laws are shown in Fig. 1(c). As shown, the modulation laws exhibit symmetric nonlinear variations about the center of the pulse and the exact shape, as rigorously defined by equation (12) which sets the instantaneous frequency variation within the pulse width, can be generated only by a programmable DDS scheme. Such advanced matched filtering does not add any additional overhead compared to the use of conventional linear chirping both in terms of hardware and software. The shift from LFM to NLFM is made by merely switching the pulse waveform type in the DDS module while keeping the same pulse & fiber backscattering response characterization and matched filtering operations.

Subsequently, a measurement of the φ-OTDR response near the 50-cm span was made when using an NLFM pulse, while keeping all measurement parameters including optical power and RF inputs the same as that of the LFM pulse. The plot of the variation of the matched filter output when using LFM and NLFM probes are given in Fig. 8, which shows the compressed responses relative to the trace levels normalized to the respective peaks. It is worth noting that the response using NLFM has enhanced resolution of the positions of the patch cord, with reflections from the connectors at both ends of the patch cord clearly visible.

The response also exhibits suppression of compression sidelobes compared to conventional compression with the LFM before, within and after the position of the patch cord. Note that the use of such reflections, which are a priori known to happen at a fixed physical point on the fiber, is the best benchmark for making sure the responses of spatially resolved measurements correspond to the actual events, and one of the conclusions from our observation is that linear chirping of a pulse introduces such errors. The source of the reduced ambiguity in compressed φ-OTDR responses is the advanced filtering with DDS-generated NLFM pulses generated with the flexible and readily adaptable DDS technique. This has been confirmed with the comparison of the relative power levels in the sideways oscillations with respect to the respective main lobe levels at the peaks of the ACFs of both the LFM and NLFM probes, which are shown in Fig. 9. Despite the fact that neither averaging is done nor other optimizations are employed, the sidelobe levels are significantly lower than the peak for the nonlinear chirp compared to that of the linear one, with the effective sidelobe suppression being $\sim$20 dB for the NLFM probe, for an improvement of $\sim$16 dB with respect to that of the LFM. To quantitatively assess the benefit of reduced range ambiguity with the proposed method, a comparison of the suppression of the sidelobes in the compressed responses for a pair of reflective events placed 0.5 m apart at $\sim$1.13 km for an NLFM probe with respect to that of an LFM one is depicted in Fig. 10, which shows the relative power of the backscattering at both sides of the events normalized to the respective peak. This analysis also confirms that there is a significant leakage of power in the response corresponding to the sideways oscillations from an LFM pulse while, in the one obtained with the NLFM probe, they are significantly suppressed in both sides of the two reflection events. Note that such power-vs-range plot showing the relative magnitude of the compressed signal over a large scale around localized events is a key aspect of pulse compression schemes used to compare the range resolution capacity of different matched filters. It can be clearly seen that the power level in the sidelobes at the sides of the connectors in the NLFM response is significantly suppressed (by up to $\sim$18 dB below the main lobe), further confirming the presence of attenuated crosstalk among signals from adjacent positions along the fiber.

Thus, the use of a readily customizable DDS addresses a key issue of reducing ambiguity in spatially resolved measurements in time domain reflectometry and it can be flexibly adapted to any given application. Our observations show that linear frequency modulation used in conventional pulse compression schemes results in increased sidelobes in compressed responses, and that advanced filtering techniques which have widely been used in radiofrequency applications can also be flexibly employed in

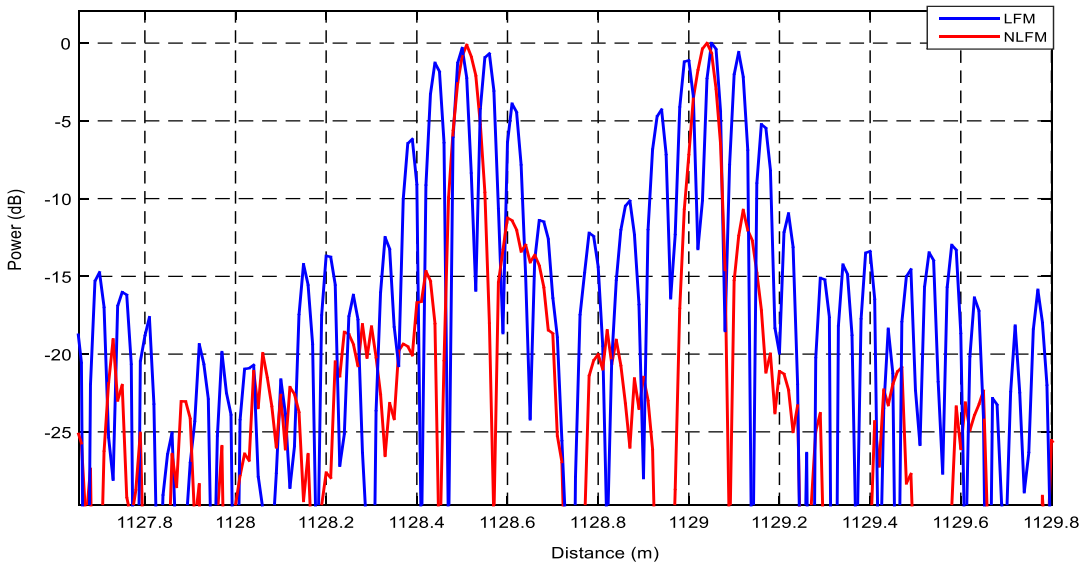

Fig. 10. Relative power of the compressed response near a 0.5 m event showing significant suppression of the contributions of sidelobes in the backscattering using NLFM.

fiber-optic systems to address this issue without adding overheads of cost and complexity compared to existing systems. The adaptability of the proposed technique contributes to ongoing efforts to make time-domain schemes competitive with frequency and correlation domain techniques in terms of offering spatially resolved measurements with reduced ambiguity.

In addition, given the possibility to implement advanced matched filtering using IFFT implemented with fast processors and FPGAs, the proposed scheme also offers possibilities to reduce range ambiguity at longer distances with enhanced speed. With respect to the mechanism of denoising used in the proposed method, it is worth noting that a matched filter is in general aimed at maximizing the SNR at the output with respect to AWGN. In our case, the system is the FUT and the input is the optical pulse probe sent into the fiber. Hence, a filter matched to the input, which is the probe sent into the optical fiber, needs to be used. For longer fibers, although the presence of nonlinear effects introducing non-AWGN noise may inevitably affect the SNR of the measurement, the AWGN contribution of the far end of the fiber will still be suppressed with the matched filtering.

Note also that performing N averages can improve the SNR by $\sqrt{N}$ but reduces the effective sampling rate, and hence the measurable frequency of vibration, by a factor of N. The achievable spatial resolution is dependent on the total bandwidth of the pulse and modulation values of a few tens of GHz can give rise to sub-centimeter resolutions. Besides, the signal processing for advanced pulse compression comprises of cross-correlation operations between the matched filter and the raw, uncompressed signal, which can be efficiently implemented with FFT operations. FPGA-based signal processing schemes, which have been used to enhance FFT processing rates for radiofrequency systems with frequency-modulated continuous waveforms by up to 7.3 times [28], can also be employed in optical pulse compression to enable more efficient denoising of backscattering traces.

V. Conclusion

In summary, we have proposed and experimentally demonstrated a φ-OTDR scheme for enhanced spatially resolved measurements using a dynamically adaptable frequency modulation scheme based on direct digital synthesis of chirps with custom, easily programmable modulation laws suitable for advanced matched filtering. The use of DDS has been shown to provide high fidelity of chirp waveforms for pulse compression in improving range resolution in a manner which is not strictly tied to specific electronic or optical components in the sensing scheme. Experimental results confirm that significantly suppressed range ambiguity is observed when compressing a 1.2-μs pulse to resolve a 50-cm event at ∼1.13 km with no averages in acquired traces, thanks to enhanced features of the autocorrelation function of the DDS-generated NLFM pulse offering optical sidelobe suppression of ∼20 dB, with an improvement of ∼16 dB compared to the use of a conventional LFM pulses. A quantitative comparison of the spatial distributions of the power of localized events in the power-range plots of compressed responses shows that nonlinear chirping of the probe results in significant suppression of event ambiguity compared to conventional linear chirping by up to ∼18 dB.

The proposed pulse compression technique, which involves a modulation law with a rigorously defined nonlinear function suitable for bandwidth-limited synthesis of waveforms optimized for sidelobe suppression, allows enhancing spatially resolved measurements by mitigating range ambiguity in phase-sensitive optical time domain reflectometry with widely available DDS components. The demonstrated flexibility of the generation of the probe and pulse optical compression can also be employed in dynamically changing the spatial resolution and adding new features providing other benefits without changing the overall cost and physical configuration of the system.

REFERENCES

[1] Y. Muanenda, C. J. Oton, and F. Di Pasquale, "Application of Raman and Brillouin scattering phenomena in distributed optical fiber sensing," *Front. Phys.*, vol. 7, 2019, Art. no. 155.

[2] Y. Muanenda, "Recent advances in distributed acoustic sensing based on phase-sensitive optical time domain reflectometry," *J. Sensor*, vol. 2018, pp. 1–16, 2018.

[3] Y. Muanenda, S. Faralli, C. J. Oton, C. Cheng, M. Yang, and F. Di Pasquale, "Dynamic phase extraction in high-SNR DAS based on UWF-BGs without phase unwrapping using scalable homodyne demodulation in direct detection," *Opt. Exp.*, vol. 27, no. 8, pp. 10644–10658, 2019.

[4] W. Zou, S. Yang, X. Long, and J. Chen, "Optical pulse compression reflectometry: Proposal and proof-of-concept experiment," *Opt. Exp.*, vol. 23, no. 1, pp. 512–522, 2015.

[5] A. Coscetta *et al.*, "Wind turbine blade monitoring with Brillouin-based fiber-optic sensors," *J. Sensor*, vol. 2017, pp. 1–5, 2017.

[6] S. Lomperski, C. Gerardi, and W. D. Pointer, "Fiber optic distributed temperature sensor mapping of a jet-mixing flow field," *Exp. Fluids*, vol. 56, no. 3, 2015.

[7] H. J. Bang, M. Jang, and H. Shin, "Structural health monitoring of wind turbines using fiber Bragg grating based sensing system," in *Proc. Sensors Smart Structures Technol. for Civil, Mech., Aerosp. Syst.*, 2011, Art. no. 7981.

[8] A. Catalano *et al.*, "An optical fiber intrusion detection system for railway security," *Sensors Actuators A Phys.*, vol. 253, pp. 91–100, 2017.

[9] G. Allwood, G. Wild, and S. Hinckley, "Optical fiber sensors in physical intrusion detection systems: A review," *IEEE Sens. J.*, vol. 16, no. 14, pp. 5497–5509, Jul. 2016.

[10] B. Lu *et al.*, "High spatial resolution phase-sensitive optical time domain reflectometer with a frequency-swept pulse," *Opt. Lett.*, vol. 42, no. 3, pp. 391–394, 2017.

[11] W. Zou, S. Yang, X. Long, and J. Chen, "Optical pulse compression reflectometry with 10 cm spatial resolution based on pulsed linear frequency modulation," in *Proc. Opt. Fiber Commun. Conf.*, 2015, paper W3I.5.

[12] M. A. Richards, *Fundamentals of Radar Signal Processing*, 2nd ed.,New York, NY, USA: McGraw-Hill Education, 2005.

[13] J. Pastor-Graells *et al.*, "SNR enhancement in high-resolution phase-sensitive OTDR systems using chirped pulse amplification concepts," *Opt. Lett.*, vol. 42, no. 9, pp. 1728–1731, 2017.

[14] C. Leśnik, "Nonlinear frequency modulated signal design," *Acta Physica Polonica*, vol. 116, no. 3, pp. 351–354, 2009.

[15] I. C. Vizitiu, "Some aspects of sidelobe reduction in pulse compression radars using NLFM signal processing," *Prog. Electromagn. Res. C PIER C*, vol. 47, pp. 119–129, 2014.

[16] I. Gladkova, "Design of frequency modulated waveforms via the Zak transform," *IEEE Trans. Aerosp. Electron. Syst.*, vol. 40, no. 1, pp. 355–359, Jan. 2004.

[17] C. Skach and S. Noorizadeh, "How new DAC technologies are changing signal generation for test," Electronicdesign.com, May 10 2017. [Online]. Available: https://bit.ly/35dxalj

[18] S. Zahrai and M. Onabajo, "Review of analog-to-digital conversion characteristics and design considerations for the creation of power-efficient hybrid data converters," *J. Low Power Electron. Appl.*, vol. 8, no. 2, pp. 12, 2018.

[19] Y. Muanenda, S. Faralli, P. Velha, C. Oton, and F. Di Pasquale, "A novel pulse compression scheme in coherent OTDR using direct digital synthesis and nonlinear frequency modulation," in *Lecture Notes in Electrical Engineering*, Cham: Springer International Publishing, 2021, pp. 173–181.

[20] D. Grodensky, "Laser ranging using incoherent pulse compression techniques," Ph.D. dissertation, Bar-Ilan Univ., Ramat-Gan, Israel, 2014.

[21] J. J. Mompó, S. Martín-López, M. González-Herráez, and A. Loayssa, "Sidelobe apodization in optical pulse compression reflectometry for fiber optic distributed acoustic sensing," *Opt. Lett.*, vol. 43, no. 7, pp. 1499–1502, 2018.

[22] M. Sagues, E. Piñeiro, E. Cerri, A. Minardo, A. Eyal, and A. Loayssa, "Two-wavelength phase-sensitive OTDR sensor using perfect periodic correlation codes for measurement range enhancement, noise reduction and fading compensation," *Opt. Exp.*, vol. 29, no. 4, pp. 6021–6035, 2021.

[23] J. J. Mompo, L. Shiloh, N. Arbel, N. Levanon, A. Loayssa, and A. Eyal, "Distributed dynamic strain sensing via perfect periodic coherent codes and a polarization diversity receiver," *J. Lightw. Technol.*, vol. 37, no. 18, pp. 4597–4602, 2019.

[24] T. D. Bhatt, "Construction of perfect periodic binary sequences for radar applications," *Int. J. Emerg. Technol.*, vol. 11, no. 2, pp. 662–667, 2020.

[25] Z. Ma *et al.*, "Phase drift noise suppression for coherent-OTDR sensing based on heterogeneous dual-sideband LFM pulse," *Appl. Phys. Exp.*, vol. 13, no. 8, 2020, Art. no. 082002.

[26] H. M. Ogden, M. J. Murray, J. B. Murray, C. Kirkendall, and B. Redding, "Frequency multiplexed coherent φ-OTDR," *Sci. Rep.*, vol. 11, no. 1, 2021, Art. no. 17921.

[27] J. Zhang *et al.*, "80 km fading free phase-sensitive reflectometry based on multi-carrier NLFM pulse without distributed amplification," *J. Lightw. Technol.*, vol. 37, no. 18, pp. 4748–4754, 2019.

[28] J. Heo, Y. Jung, S. Lee, and Y. Jung, "FPGA implementation of an efficient FFT processor for FMCW radar signal processing," *Sensors*, vol. 21, no. 19, 2021, Art. no. 6443.